European Polymer Journal 53 (2014) 292–301

Contents lists available at ScienceDirect

European Polymer Journal

journal homepage: www.elsevier.com/locate/europolj

Macromolecular Nanotechnology

Graphene nanoplatelets thickness and lateral size influence on the morphology and behavior of epoxy composites

S.G. Prolongo *, A. Jiménez-Suárez, R. Moriche, A. Ureña

Dpt. Materials Science and Engineering, University Rey Juan Carlos, C/Tulipán s/n, Móstoles, 28933 Madrid, Spain

ARTICLE INFO

Article history:
Received 15 October 2013
Received in revised form 8 January 2014
Accepted 14 January 2014
Available online 28 January 2014

Keywords:
A. Polymer–matrix composites (PMCs)
A. Thermosetting resin
B. Microstructures
B. Thermomechanical

ABSTRACT

Graphene nanoplatelets/epoxy nanocomposites were prepared using a high shear toroidal mixer as dispersion technique. Suitable dispersions were obtained. Several graphene nanoplatelets, with different thickness and lateral dimensions, were added in order to analyze the influence of these parameters in the final properties. An important nanofiller concentration gradient was found from the top to the bottom in nanocomposites reinforced with large nanoplatelets due to a natural deposition by gravity. This phenomenon is not appreciable when the nanoplatelets size decreased. However, the small nanoplatelets have a greater tendency to agglomerate in packages of several parallel particles. In general, graphene nanoplatelets addition caused an increment in glass transition temperature, stiffness and thermal stability compared to the epoxy resin. However, it was also found that graphene nanoplatelets dimensions significantly affect to these enhancements. Nanocomposites reinforced with larger and thicker nanoplatelets presented lower glass transition temperature, higher modulus and higher decomposition temperature.

1. Introduction

Graphene is a two-dimensional material consisting of sp^2-hybridized carbon atoms arranged in a honeycomb structure. When this material is constituted by a unique hexagonal atoms plane, it is named graphene sheet, while graphene nanoplatelets refer to particles with a nanometric thickness, in the range of 3–100 nm (GNPs) [1]. The carbon atoms are strongly bonded in a hexagonal plane but weakly bonded normal to the plane. Nowadays, the use of these materials as polymer fillers is being widely studied [2–4]. It is expected that graphene reinforced polymer composites show important improvements in their mechanical properties, electrical and thermal conductivity and other thermophysical properties [5,6]. Another advantage is that the 2-dimensional nanoplatelet can increase the gas permeation resistance of polymer composites [7]. These improvements can be maximized when graphene is exfoliated in an isolated layer and the morphology of the composites is tailored as dispersed and stretched particles in order to obtain the highest aspect ratio.

Great efforts have been made in processing of graphene/polymer composites. The van der Waals forces are the main problem of graphene dispersion and, consequently, the π–π inter-planar stacking. Most of the processing techniques are based on graphene solutions or dispersions, either in water or organic solvent [8]. However, one of the main challenges to achieve the large-scale potential for technological and engineering applications is to homogeneously disperse thin graphene nanoplatelets within the polymer matrix. Micro-mechanical dispersion and exfoliation can help to motivate research towards a scalable procedure without using intercalants. Following the developed methodology for manufacturing carbon nanotube reinforced polymers, calandering technique

* Corresponding author. Tel.: +34 914888292; fax: +34 914888150.
E-mail address: silvia.gonzalez@urjc.es (S.G. Prolongo).

http://dx.doi.org/10.1016/j.eurpolymj.2014.01.019
0014-3057/

using the three-roll mill has been used in graphene/polymer composites processing [9]. Suitable dispersions have been reported for composites with epoxy matrices [10–12]. Another technique, less studied than the previous one but also based on shear micromechanical forces, is the high shear-speed mixing. No research has been found about the use of this technique in the manufacturing of graphene/epoxy composites. Its main advantage is its capability of being industrially scaled up. Also, it is probed that it allows obtaining nanofillers homogeneous dispersions, as in the case of carbon nanotubes [14,15]. Both of the techniques are based on applying high shear forces and therefore, it is necessary to carry out a deep study of the composites morphology, determining the final thickness and exfoliation degree of graphene nanofillers, their spatial arrangement (wrinkling or stretched) and the morphology of the composite, elucidating that way the dispersion and distribution of nanoplatelets (stacked or agglomerated).

Similar to previous researches about carbon nanotubes reinforced composites, the effect of numerous experimental conditions on the morphology and behavior when using graphene as nanofiller is not clear. Different results, even conflicting, have been published [2–4]. These differences may be associated to differences in the source and production of graphene nanofillers, e.g. mechanical milling of graphite, thermal or chemical reduction of graphene oxide, and differences in the nanocomposite manufacturing technique used. In this work, in addition to the effectiveness of the manufacturing technique, the effect of GNPs size and thickness is studied, by using nanofillers from the same source. This research is complementary to other previous published works [13,16,17].

2. Experimental

2.1. Materials

Three different types of GNPs (manufactured by Chemical Reduction) were purchased in Graphene Supermarket [18] and their main featured are shown in Table 1. The epoxy matrix is based on a monomer called Araldite LY556, which is cured with an aromatic amine Araldite XB3473 in a 100:23 M ratio. The epoxy monomer is based on diglycidyl ether of bisphenol A (DGEBA) and the amine hardener is based on aromatic amines. Both components were provided by Huntsman.

2.2. Fabrication of composites

The composites were manufactured by applying high shear mixing (Dispermat AE). The experimental procedure consisted of mixing GNPs into the neat epoxy monomer by a high-speed mixer at 6000 rpm for 15 min, reaching the optimum Doughnut effect. By reaching this Doughnut effect, the mixture flows moving downwards and upwards to the disc in a circular path. This movement provokes the appearance of areas with high and low stress what is advantageous in the way mixture is subjected to different efforts and the agglomerates are dispersed. Another advantage of the employed method is its scalability to industrial applications. Afterwards, the dispersed mixture was degassed in vacuum at 80 °C for 15 min and a stoichiometric ratio of the amine curing agent was then added at 80 °C. The applied curing treatment was carried out at 140 °C for 8 h. The cured samples were allowed to cool slowly to room temperature inside the oven. Composites with a 0.5 wt% GNPs content were produced.

2.3. Characterization

The commercial GNPs were characterized by X-ray diffraction (XRD), Scanning and Transmission Electron Microscopy (SEM and TEM) and Raman spectroscopy. XRD patterns were captured with a X'Pert PRO difractomer from Panalytical, using Cu Kα (λ = 1.5406 Å) radiation source operating at a voltage of 45 kV and 300 mA of electric current. The scanning was taken from 10° to 80° (2θ). SEM micrographs were obtained in a Hitachi S-3400-N microscope. A Phillips TEM Tecnai 20 microscope of 200 kV was used for TEM characterization. Raman spectra were recorded with Horiba Jobin–Yvon HR 800 UV and the excitation wavenumber was 632.8 nm from a He–Ne laser.

Morphology of composites was studied at different magnification levels using several microscopes: Optical (MO), Field Emission Gun Electron Scanning (FEG-SEM, Nova NanoSEM FEI 230) and Transmission Electron Microscopy (TEM, Phillips Tecnai 20). Optical microscopic analysis was carried out in a Leica DMR Optical Microscopy. Images were treated with a RGB mask "*white on black*" in order to enhance contrast between filler and matrix, using Image-Pro Plus software. For electron microscopy, samples were cut by cryomicrotomy. In addition, the obtained film was coated with a thin layer (5–10 nm) of Au (Pd) for FEG–SEM observation. The experimental conditions of the sputtering were 30 mA for 120 s (Baltec, SCD-005 sputter).

Thermal and thermomechanical behavior of composites was studied by differential scanning calorimetry (DSC), dynamic mechanical thermal analysis (DMTA) and Thermogravimetry analysis (TGA). DSC measurements were carried out in a Mettler Toledo mod. 821 apparatus, calibrated with indium and zinc. DSC test

Table 1
Main features of graphene nanoplatelets.

Graphenic nanoplatelets type	Purity (%)	Specific surface area (m/g^2)	Average flake thickness (nm)	Number of layers	Average particle lateral dimension (nm)	ID/IG Raman
A02	99.9	100	8	20–30	550 (150–3000)	0.3319
A03	99.2	80	12	30–50	4500 (1500–10000)	0.0334
A04	98.5	<15	60	150–250	3000–7000	0.1421

was carried out following the corresponding standard ISO 11357-2. Two scans were carried out at a heating rate of 10 °C/min from 20 to 300 °C. The amount of sample is in the range of 5–10 mg. Glass transition temperature (T_g) was taken at the middle point of the heat capacity change. DMTA was performed following the standard D5418-01, in dual cantilever bending mode using a DMTA Q800 V7.1 from TA Instruments. All the experiments were carried at 1 Hz frequency, by bending deformation, scanning from 20 to 250 °C using a heating rate of 2 °C/min. The dimensions of samples were $35 \times 12 \times 1.5\ mm^3$. The maximum of tan δ vs. temperature plots was used to identify the α-relaxation associated to the glass transition. Finally, TGA measurements were made in Mettler Toledo TGA/DSC, following the standard UNE-EN ISO 11358, scanning from 20 to 550 °C using a heating rate of 10 °C/min, with an amount of sample in the range of 10–15 mg.

3. Results

3.1. Characterization of graphene nanoplatelets

The main goal of this work is to determine the effect of size and thickness of graphene nanoplatelets on the processing, morphology and performance of GNP/epoxy nanocomposites. For this reason, three different commercial GNPs powders were selected. All these powders were manufactured using the same source and production methodology. The difference between them is their morphology, lateral size and thickness. Table 1 collects their principal characteristics, supplied by the manufacturer [18]. The nanoplatelets present different thickness from 8 to 60 nm, which means that the number of graphitic layers that constitutes each nanoparticle ranges from 20 to 250 layers. In addition, the size of graphitic plane varies from 550 nm to 7 μm. Both features induce changes in the specific surface area.

XRD patterns of the original powders were made in order to confirm their purity and crystalline structure. Fig. 1 shows mentioned XRD patterns, where diffraction peaks indexing is presented. The high purity of commercial powders is confirmed. The full width at half maximum (FWHM) of the peak gives information about the out of plane crystalline thickness by making use of the Scherrer equation [12]. As it is expected, the breadth of (002) peak increases from AO2 to AO4, indicating a higher number of graphitic layers per each crystalline nanoplatelet. Representative micrographs of SEM and TEM are shown in Fig. 2, in order to confirm differences in lateral dimensions and thickness of GNPs powders. AO3 and AO4 present similar surface area in plane while AO2 is smaller. Finally, the thickness of nanoplatelets is determined by TEM, where it is confirmed that AO4 are much thicker than AO2 and AO3.

Finally, the samples were analyzed by Raman spectroscopy that is a powerful tool to evaluate the crystalline, nanocrystalline and amorphous degree of graphitic based materials. Fig. 3 shows the spectra of AO2, AO3 and AO4. The vibration of sp^2-bonded carbon in a 2-dimensional hexagonal lattice results in a peak at 1590 cm^{-1} (G-band) that can be assigned to an E_{2g} mode of graphene [4,10,18–21]. While vibration of carbon atoms with dangling bond in plane terminations of disordered graphene is associated to the D-band at 1340 cm^{-1} (sp^3-hybridized carbons). This band is generally correlated with defects on graphitic structures derived from vacancies, heptagon–pentagon pairs, kinks, grain boundaries, amorphous carbon species and presence of heteroatoms [10]. The presence of D-band is attributed to defects in the disorder-induced modes. Table 1 collects the I_D/I_G ratio for all used nanoplatelets. This ratio is very low for AO3 powders, whose value is 0.033, increasing one order of magnitude, up 0.1–0.3, for AO2 and AO4, respectively. The high intensity and low peak width of G-band implies regular graphene structures. D-band intensity increases by two main reasons. The first one is the increase of dangling bonds percentage in plane terminations, which occurs in the

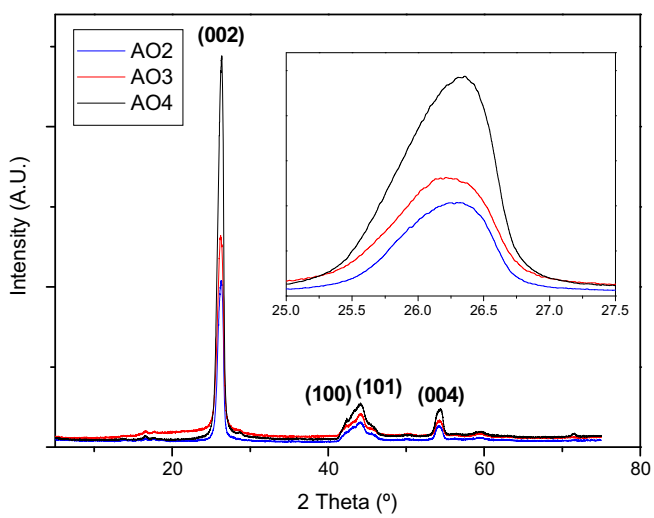

Fig. 1. DRX patterns of graphene powders. Enlargement of diffraction peak (002).

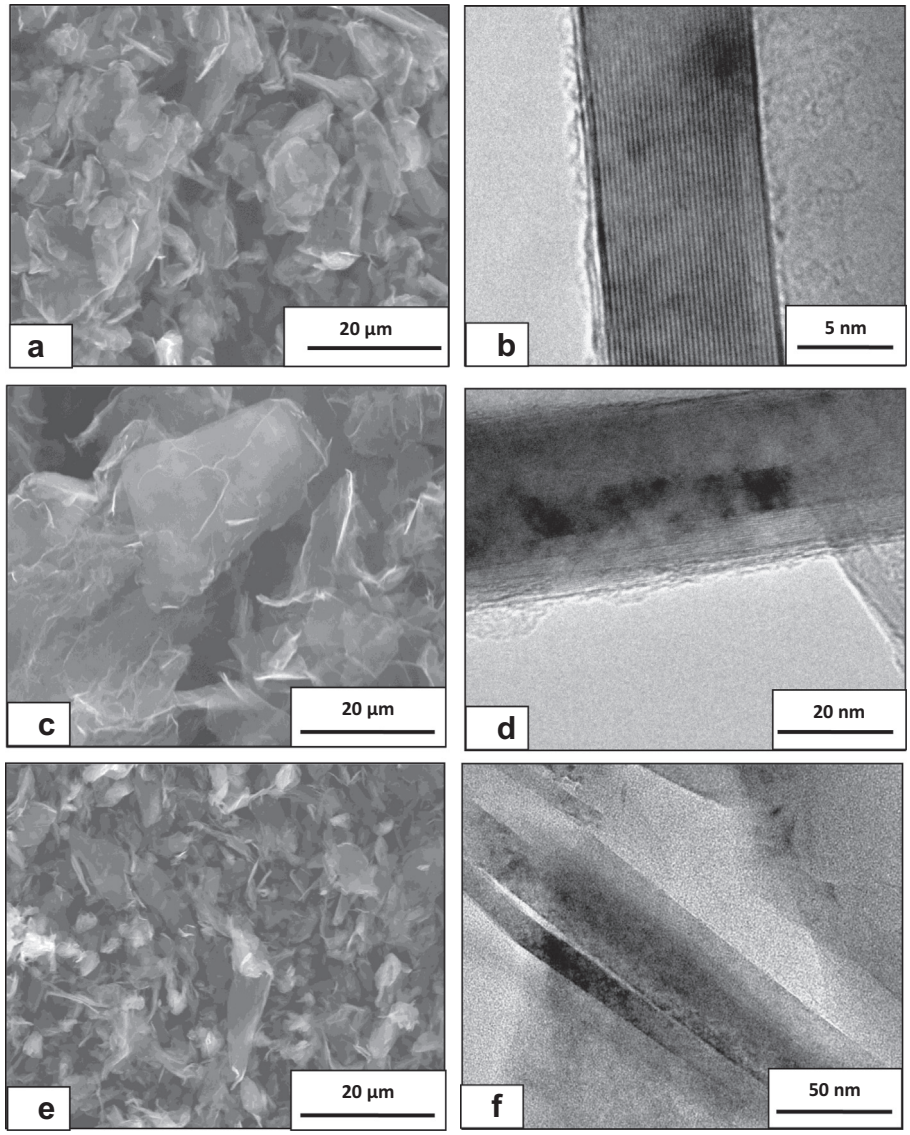

Fig. 2. SEM and TEM micrographs of graphene nanoplatelets: AO2 (a and b); AO3 (c and d) and AO4 (e and f).

smallest nanoparticles, AO2, where the sp^2/sp^3 carbon ratio is the highest. Another reason is related to the oxidation degree or the purity quality. Therefore, AO4 presents the highest number of defects on the structure. The shift of G-band at higher wavenumbers observed by AO3 and AO4 and the asymmetry of 2-D-peak shape is associated to the higher thickness of these GNPs powders, being far from a single-layer graphene [19–21].

3.2. Morphology of GNP/epoxy composites

Fig. 4 shows treated optical micrographs of the top and the bottom sides of the GNP/epoxy nanocomposites plates. Fig. 4 also presents an optical micrograph and its corresponding treated image, in order to can observe the effect of the applied mask.

It can be clearly observed that the epoxy resin reinforced with AO4 is not homogeneous, presenting a nanofiller stratification. There is a variation of the nanofillers concentration from the top to the bottom of the sample. This effect is scarcely observed in the other nanocomposites, those reinforced with AO2 and AO3. Yasmin et al. [22] have already observed this phenomenon in composites reinforced with large graphene particles due to the influence of gravity. The stratification of AO4 is associated to its high size (thickness and flake dimensions) and therefore to the high weight of particles. This stratification effect as a function of the geometry of the graphene nanoplatelets must be always considered and studied in each GNP/epoxy system because the composites with decanted nanoplateles are not homogeneous and probably present an anisotropic behavior. In order to study in depth this effect, samples with 4 mm of thickness were studied at the

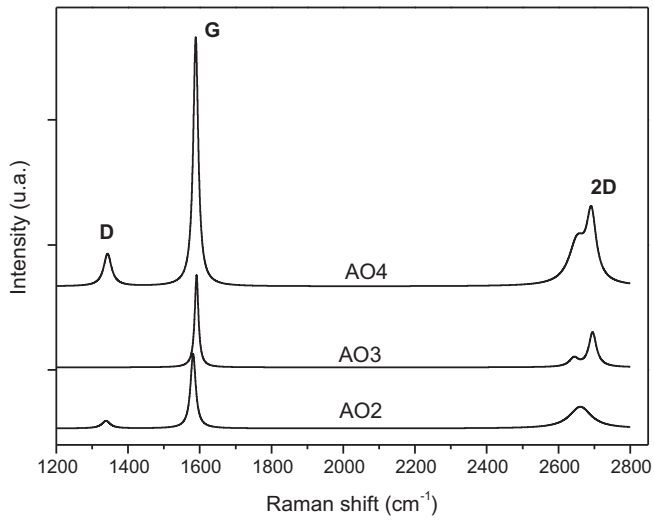

Fig. 3. Raman spectra of commercial graphene powders.

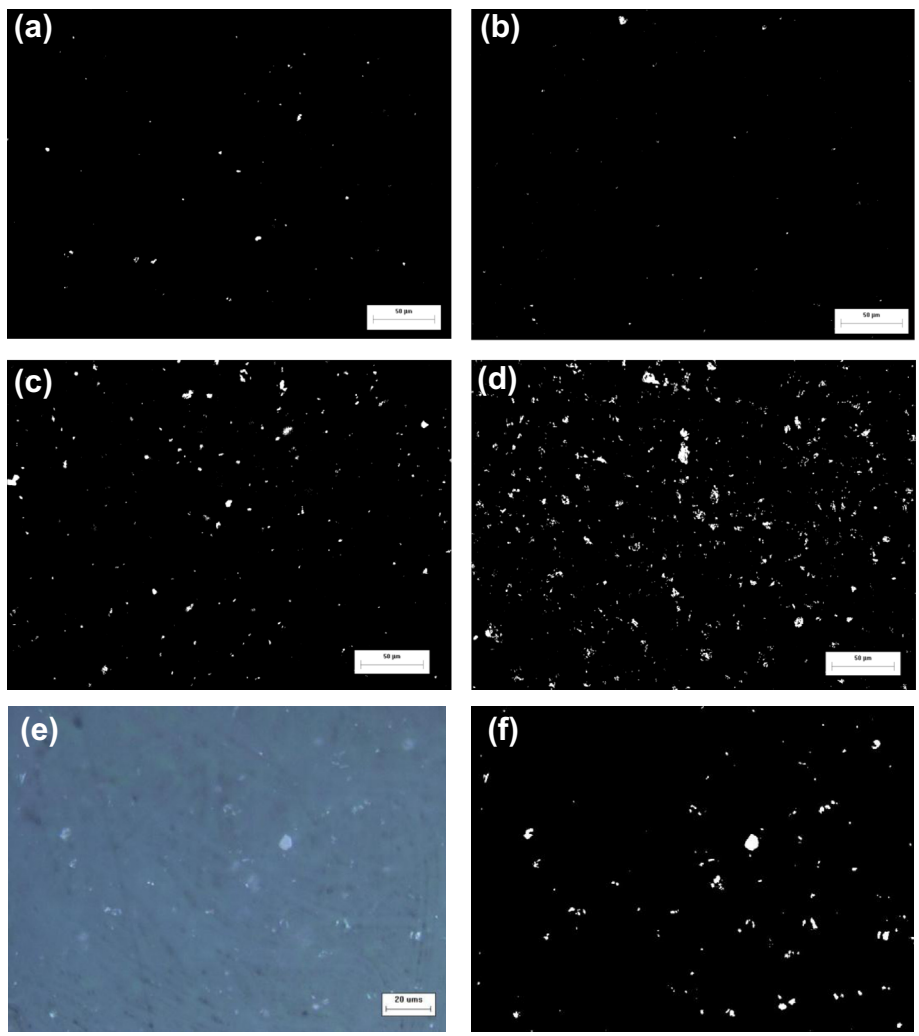

Fig. 4. Treated optical micrographs of graphene/epoxy composites reinforced with AO2, top (a) and bottom, (b), and AO4, top, (c) and bottom, (d). Fig. 4e and f shows a conventional optical micrograph of the composite and (e) and its corresponding treated image (f).

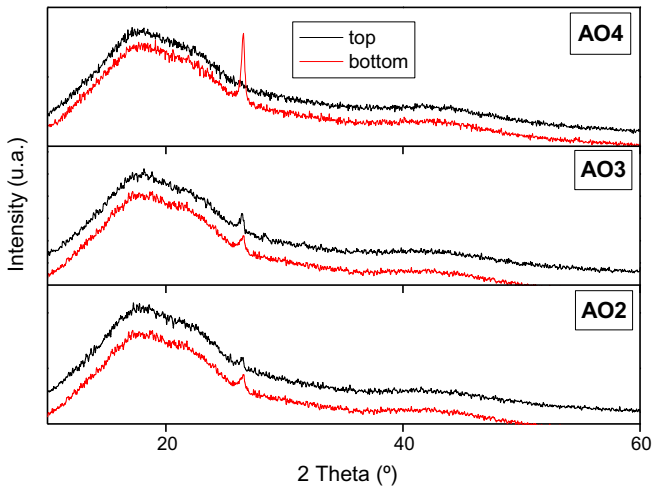

Fig. 5. XRD patterns of graphene/epoxy composites at the top and the bottom of the samples.

top and the bottom by XRD (Fig. 5). The wide diffraction from 10° to 28° is caused by scattering of cured epoxy molecules while the tiny shoulder peak found at 26.6° corresponds to the (002) graphitic plane of graphene nanoparticles [18]. Taking into account that this last peak corresponds to the interlayer distance of 3.35 Å, which is characteristic of pristine graphitic planes, its shift, widening or even modification of intensity is usually used as an indicative of intercalation or exfoliation. However, as evidenced in this work, since the diffraction intensity varies with the concentration of the crystalline features, some morphological information may be missed. In particular, Fig. 5 shows great differences in the diffraction intensity of the shoulder corresponding to (002) larger graphene nanoplatelets, AO4. It is worthy to note that the commonly used DRX analysis of GNP/epoxy composites at the top side of the samples could give misinformation about their real morphology.

The increase in size of graphene nanoparticles induces a strong decantation and that way major concentration of particles is deposited at the bottom side of the composites. Consequently, as it was observed by MO (Fig. 4), the resin filled with nanoplatelets AO4, with a high thickness and area in plane shows a high stratification degree, having most of the nanofillers at the bottom. Due to this reason, the (002) diffraction peak presents high intensity at the bottom and disappears at the top of the composite. This phenomenon is less noticeable in composites with smaller nanoparticles. AO3 is the studied nanoplatelet with an intermediate size and decantation is scarcely appreciated. The intensity of graphitic plane diffraction shoulder decreases from bottom to top. Finally, AO2, which is the smallest nanoplatelet used, with the smallest thickness and lowest flake dimensions, does not seem to present this effect. In this case, the diffraction intensity of the (002) peak is not modified along the composite thickness. Therefore, the main conclusion is that GNP/epoxy composites can present nanoparticles decantation and this phenomenon is strongly dependent on nanoparticles size, resulting in a nanofiller concentration gradient from top to bottom of the sample in composites with large and thick graphene nanoparticles. Also, XRD could give misinformation due to the concentration gradient of crystalline nanoplatelets along thickness.

On the other hand, in order to analyze the efficiency of the dispersion technique, samples were observed by FEG-SEM (Fig. 6). The presented micrographs corroborate that the nanoplatelets were not exfoliated or intercalated. Without considering the AO4 decantation, a suitable dispersion of nanoparticles into the epoxy matrix is observed. In general, graphene nanoplateles are homogenously dispersed with a similar distance between each other, confirming the efficiency of the dispersion technique. However, packaging of parallel nanoplatelets were found for composites reinforced with the smallest graphene nanoparticles, AO2 (Fig. 6b). This stacking is associated to the large aspect ratio of the nanofiller [20]. It can be also observed a preferential orientation of the platelets (Fig. 6d), flakes are directed parallel to the axis *x*–*y*. Additionally, for all the studied composites, it is interesting to observe that all the nanoplatelets, even the thickest ones, are stretched, without wrinkling and rolling effects (Figs. 6b and d). As well, a weak interface is observed (Fig. 6b and d) due to the fact that the added nanofillers are not functionalized. Both phenomena will have to be studied in future researchers.

3.3. Thermal and thermo-mechanical behavior of GNP/epoxy composites

In order to study the influence of the graphene nanoplatelets addition on the behavior of the epoxy resin, the composites were analyzed by DSC, TGA and DMTA. Due to the concentration gradient of nanoplatelets explained in the previous section, the presented results are average values of the measurements that have been carried out at the top and the bottom of the samples. The obtained results are collected in Table 2 and the experimental curves are collected in Fig. 7.

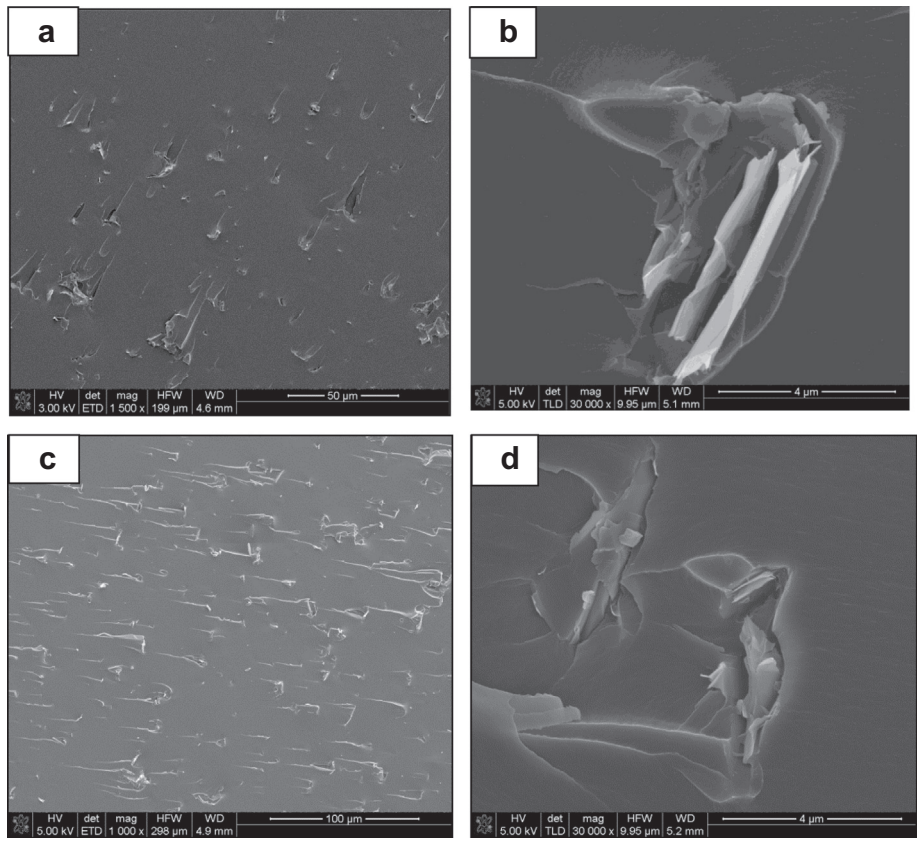

Fig. 6. High magnification FEG-SEM images of graphene/epoxy composites reinforced with AO2 (a and b) and AO4 (c and d).

Table 2
Thermal and dynamo-mechanical results of neat epoxy resin and composites reinforced with graphene nanoplatelets.

	DSC		TGA		DMTA		
	T_g^1 (°C)	T_g^2 (°C)	T_d (°C)	Degradation rate (mg/°C)	E'_G (GPa)	E'_R (MPa)	T_α (°C)
Neat epoxy	152	158	415	0.441	2.34	20.00	163
AO2	162	165	417	0.352	2.19	33.56	171
AO3	155	157	419	0.327	1.34/2.18	16.80	169/158
AO4	148	156	422	0.309	2.30	29.10	160

T_g^1: Glass transition temperature measured in first DSC scan.
T_g^2: Glass transition temperature measured in second DSC scan.
T_d: Degradation temperature measured by TGA.
E'_G : Storage modulus in glassy state at 30 °C measured by DMTA.
T_α: α-relaxation temperature measured by DMTA as maximum of tan δ peak.

The size of graphene nanoplatelets, as it has been also reported by Thanh et al. [23], plays an important role in T_g values measured by both techniques, DSC and DMTA (Table 2). The T_g of composites reinforced with the smallest studied nanofiller, AO2, is 10 °C higher than that one of the pristine resin. This result is promising regard to clay/epoxy composites, where an important decrease of T_g is measured by addition of this 2-D inorganic nanofiller [24]. In general, a T_g increase in any polymeric system reinforced with nanofillers is associated with restriction in molecular motion and reduction in the free volume, impeding polymer chain mobility [25,26]. The increase of T_g indicates an effective arrangement of graphene nanoplatelets in the epoxy matrix so that the nanometer particle size can constrain the segmental motion of cross-links. A major thickness and flake size of nanoparticles induces a decrease of T_g improvement. In fact, composite reinforced with AO3 presents a T_g value similar to that one of the neat epoxy resin while the T_g of composites reinforced with AO4 is even lower. It is known [27,28] that there are numerous factors that can affect T_g, such as dispersion degree, homogeneity, spacing between particles, as well as size of nanoparticles. Several authors have confirmed that the addition of relative large particles has no influence on the T_g of the com-

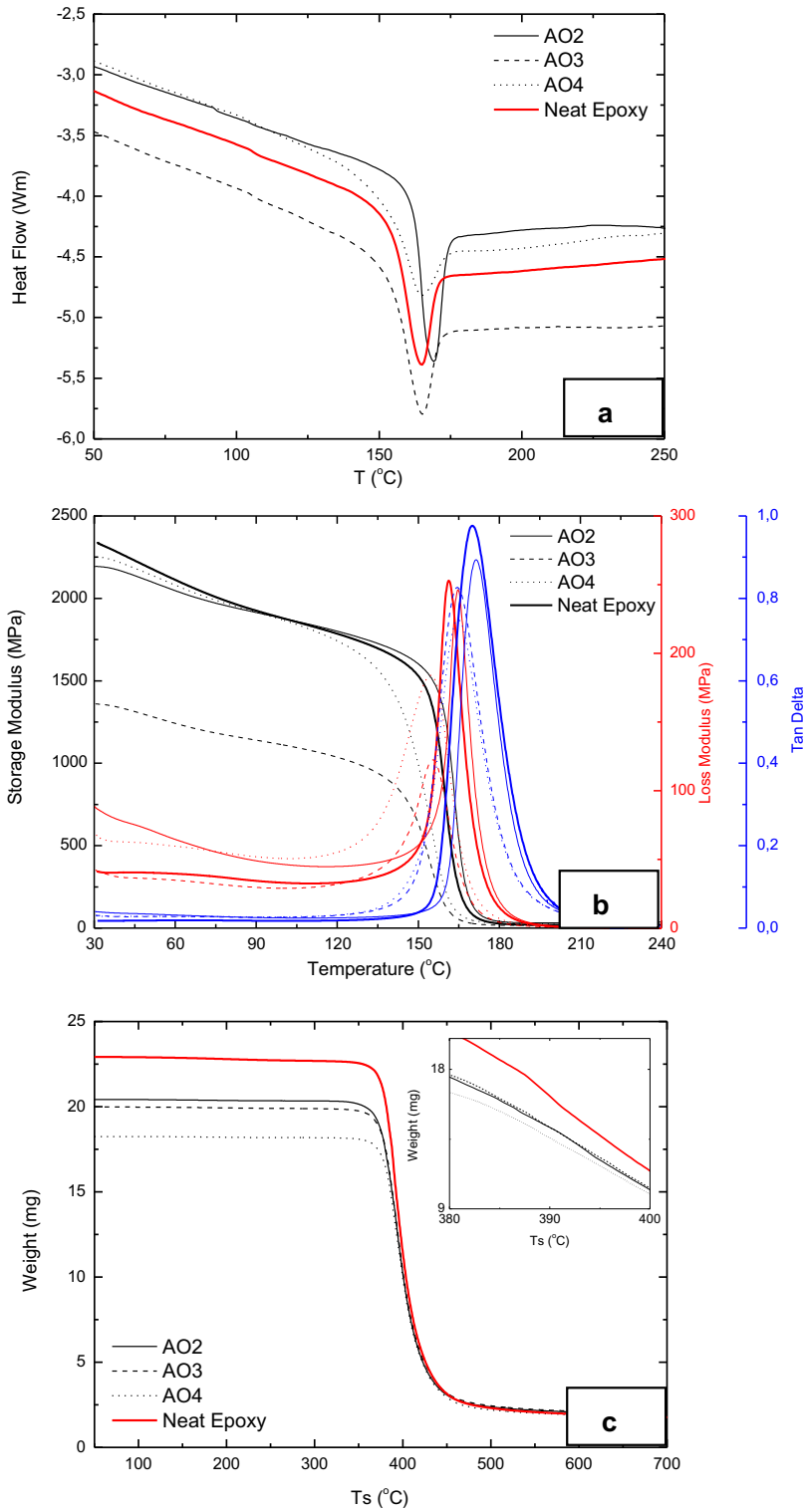

Fig. 7. Thermal characterization of the neat epoxy resin and graphene/epoxy composites. Curves of DSC (a), DMTA (b) and TGA (c).

posite polymers [28]. In addition, it has been demonstrated that thermal conductivity of graphene nanoplatelets and, therefore their corresponding composites, is proportionally reduced with the layer size [16].

Defect-free graphene is the stiffest material ($E \sim 1$ TPa) ever reported in nature. Because of this, the storage modulus increase, measured in the glassy region, of the corresponding composites is evident. In fact, the light increase

measured in the manufactured composites must be associated with a weak interface, limiting the load transfer between matrix and nanoplatelets. The stiffness enhancement increases with the GNPs size, being higher for the composites with larger nanoplatelets. AO3 and AO4 present a higher flake size. These results are in full agreement with the work published by Coleman and coworkers [29]. They found that for a given loading of graphene, the reinforcement effect decreases as the graphene flake size diminishes. This is consistent with the findings of Gong et al. [30] who conclude the need to have large lateral graphene flake dimensions in order to have a suitable reinforcement.

Not great differences are observed in the value of storage modulus in the rubbery state at high temperature, meaning that the crosslinking degree of the matrix is similar in all studied composites.

Finally, the TGA results clarify that the incorporation of graphene nanoplatelets induces a slight thermal stabilization. This enhancement can be attributed to the so-called "tortuous" path effect, which delayed the escape of volatile degradation products and also char formation [31,32]. The graphene nanoplatelets prevent the emission of small gaseous molecules during thermal degradation and can also disrupt the oxygen supply by forming charred layers on the surface of the composites. This indicates that GNPs can act as a good barrier to prevent degradation of polymers. The variation of degradation temperature is not large due to the fact that graphene nanoplatelets are not exfoliated and therefore their specific surface area is not so high. It is worthy to note that the addition of graphene induces a double positive effect in the thermal behavior of epoxy resin: an increase of the degradation temperature and a decrease of the degradation rate. Both parameters depend on the flake size of nanoplatelets. The degradation temperature increases while simultaneously the degradation rate decreases as the flake size of nanoplatelets increases, due to their higher efficiency to form tortuous paths.

4. Conclusions

GNP/epoxy nanocomposites were prepared using high-shear toroidal mixer as dispersion technique. Its main advantage is its simplicity, production rate, and easy implementation at industrial scale, regard other more common dispersion techniques, such as ultrasonication or three roll mixer. The composites presented a suitable dispersion of graphene nanoplatelets, with homogenous space between particles. However, an important concentration gradient was found from the top to the bottom of the sample for composites with larger and thicker nanoplatelets. Therefore, the addition of thick graphene nanoplatelets implies the appearance of phenomenon of self-decantation.

The epoxy composites reinforced with graphene nanoplatelets present enhanced mechanical and thermal properties, showing a simultaneous increase of several parameters, such as the glass transition temperature, the storage modulus at room temperature and the degradation temperature.

Three different graphene nanoplatelets, with different thickness and flake size, were added in order to analyze the influence of the size of the nanofiller: thickness and lateral dimensions. The main conclusions drawn can be summarized in:

(a) The increase of nanoparticles weight, increasing their thickness and flake size, induces an important self-decantation phenomenon. The composites show a concentration gradient along the composite thickness due to the gravity effect, leading heterogeneous and stratifying materials.
(b) The decrease of nanoparticles size enhances the stacking of nanoplatelets due to the highest aspect ratio and specific surface area.
(c) The increase of nanoparticles dimensions decreases the enhancement of glass transition temperature because larger filler cannot affect to local mobility of polymeric segments between crosslinking knots.
(d) The increase of lateral dimensions of nanoplatelets gives higher thermal stability to the corresponding composites, increasing the degradation temperature and decreasing the degradation rate.

Acknowledgements

The authors wish to thank the Ministerio de Economia y Cometitividad of Spain Government (Project MAT2013-46695-C3-1-R) and IBERDROLA Foundation, through its Call for Research on Energy and the Environment Grants "ENERGY FOR RESEARCH".

References

[1] Chu K, Li W, Dong H. Role of graphene waviness on the thermal conductivity of graphene composites. Appl Phys A 2013;111:221–5. http://dx.doi.org/10.1007/s00339-012-7497-y.
[2] Kim H, Abdale AA, Macosko CW. Graphene/polymer nanocomposites. Macromolecules 2010;43:6515–30. http://dx.doi.org/10.1021/ma100572e.
[3] Juilla T, Bhadra S, Yao D, Kim NH, Bosem S, Lee JH. Recent advances in graphene based polymer composites. Prog Polym Sci 2010;35:1350–75. http://dx.doi.org/10.1016/j.progpolymsci.2010.07.005.
[4] Mahmoud WE. Morphology and physical properties of poly(ethylene oxide) loaded graphene nanocomposites prepared by two different techniques. Eur Polym J 2011;47(8):1534–40. http://dx.doi.org/10.1016/j.eurpolymj.2011.05.011.
[5] An J, Gyu Jeong Y. Structure and electric heating performance of graphene/epoxy composite films. Eur Polym J 2013;49:1322–30. http://dx.doi.org/10.1016/j.eurpolymj.2013.02.005.
[6] Martin-Gallego M, Bernal MM, Hernandez M, Verdejo R, Lopez-Manchado MA. Comparison of filler percolation and mechanical properties in graphene and carbon nanotubes filled epoxy nanocomposites. Eur Polym J 2013;49:1347–53. http://dx.doi.org/10.1016/j.eurpolymj.2013.02.005.
[7] Galpaya D, Wang M, Liu M, Motta N, Waclawik E, Yan C. Recent advances in fabrication and characterization of graphene–polymer nanocomposites. Graphene 2012;1:30–49. http://dx.doi.org/10.4236/graphene.2012.12005.
[8] Li D, Müller MB, Gilje S, Kaner RB, Wallace GG. Processable aquous dispersions of graphene nanosheets. Nat Nanotechnol 2008;3:101–5. http://dx.doi.org/10.1038/nnano.2007.451.
[9] Hamilton CE, Lomeda JR, Sun Z, Tour JM, Barron AR. High-yield organic dispersions of unfunctionalized graphene. Nano Lett 2009;9:3460–2. http://dx.doi.org/10.1021/nl9016623.
[10] Raza MA, Westwood AVK, Brown AP, Stirling C. Texture, transport and mechanical properties of graphite nanoplatelets/silicone

composites produced by three roll mill. Compos Sci Technol 2012;72:467–75. http://dx.doi.org/10.1016/j.compscitech.2011.12.010.
[11] Chatterjee S, Wang JW, Kuo WS, Tai NH, Salzmann C, Li WL, et al. Mechanical reinforcement and thermal conductivity in expanded graphene nanoplatelets reinforced epoxy composites. Chem Phys Lett 2012;531:6–10. http://dx.doi.org/10.1016/j.cplett.2012.02.006.
[12] Chatterjee S, Nafezarefi F, Tai NH, Shlagenhauf L, Hüesch FA, Chu BTT. Size and synergic effects of nanofiller hybrids including graphene nanoplatelets and carbon nanotubes in mechanical properties of epoxy composites. Carbon 2012;50:5380–6. http://dx.doi.org/10.1016/j.carbon.2012.07.021.
[13] Gojny FH, Wichmann MHG, Fiedler B, Schulte K. Influence of different carbon nanotubes on the mechanical properties of epoxy matrix composites – a comparative study. Compos Sci Technol 2005;65:2300–13. http://dx.doi.org/10.1016/j.compscitech.2005.04.021.
[14] Tang LC, Zhang H, Han JH, Wub XP, Zhang Z. Fracture mechanisms of epoxy filled with ozone functionalized multi-wall carbon nanotubes. Compos Sci Technol 2011;72:7–13. http://dx.doi.org/10.1016/j.compscitech.2011.07.016.
[15] Martin CA, Sandler JKV, Shaffer MSP, Schwarz MK, Bauhofer W, Schulte K, et al. Formation of percolating networks in multi-wall carbon-nanotube-epoxy composites. Compos Sci Technol 2004;2004(64):2309–16. http://dx.doi.org/10.1016/j.compscitech.2004.01.025.
[16] Cao HY, Guo ZX, Xiang H, Gong XG. Layer and size dependence of thermal conductivity in multilayer graphene nanorribbons. Phys Lett A 2012;376:525–8. http://dx.doi.org/hysleta.2011.11.016.
[17] Chirtoc M, Horny N, Tavman I, Turgut A, Kökey I, Omastová M. Preparation and photothermal characterization of nanocomposites based on high density polyethylene filled with expanded and unexpanded graphite: particle size and shape effects. Int J Therm Sci 2012;62:50–5. http://dx.doi.org/10.1016/j.ijthermalsci.2012.02.015.
[18] https://graphene-supermarket.com/.
[19] Clark SM, Jeon KJ, Chen JY, Yoo CS. Few layer graphene under high pressure: Raman and X-Ray diffraction studies. Solid State Commun 2013;154:15–8. http://dx.doi.org/10.1016/j.ssc.2012.10.002.
[20] Yang SY, Lin WN, Huang YL, Tien HW, Wang JY, Ma CCM, et al. Synergic effects of graphene platelets and carbon nanotubes on the mechanical and thermal properties of epoxy composites. Carbon 2011;49:793–803. http://dx.doi.org/10.1016/j.carbon.2010.10.014.
[21] Tien DH, Park J, Han SA, Ahmad M, Seo Y. Electrical and thermal conductivities of stycast 1266 epoxy/graphite composites. J Korean Phys Soc 2011;59:2760–4. http://dx.doi.org/10.3938/jkps.59.2760.
[22] Yasmin A, Luo JJ, Daniel IM. Processing of expanded graphite reinforced polymer nanocomposites. Compos Sci Technol 2006;66:1182–9. http://dx.doi.org/10.1016/j.compscitech.2005.10.014.
[23] Thanh TD, Kaprálková L, Hromádková J, Kelnar I. Effect of graphite nanoplatelets on the structure and properties of PA6-elastomer nanocomposites. European Polymer Journal, in press. http://dx.doi.org/10.1016/j.eurpolymj.2013.10.022.
[24] Azeez AA, Rhee KY, Park SJ, Hui D. Epoxy clay nanocomposites – processing, properties and applications. A Rev Compos: Part B 2013;45:308–20. http://dx.doi.org/10.1016/j.compositesb.2012.04.012.
[25] Yasmin A, Daniel IM. Mechanical and thermal properties of graphite platelet/epoxy composites. Polymer 2004;45:8211–9. http://dx.doi.org/10.1016/j.polymer.2004.09.054.
[26] Becker O, Varley R, Simon G. Morphology, thermal relaxations and mechanical properties of layered silicate nanocomposites based upon high-functionality epoxy resins. Polymer 2002;43:4365–73. http://dx.doi.org/10.1016/S0032-3861(02)00269-0.
[27] Kim J, Yim BS, Kim JM, Kim J. The effects of functionalized graphene nanosheets on the thermal and mechanical properties of epoxy composites for anisotropic conductive adhesives (ACAs). Microelectron Reliab 2012;52:595–602. http://dx.doi.org/10.1016/j.microrel.2011.11.002.
[28] Xiong M, Cu G, You B, Wu L. Preparation and characterization of poly(styrenebutylacrylate) latex/nano-ZnO nanocomposites. J Appl Polym Sci 2003;90:1923–31. http://dx.doi.org/10.1002/app.12869.
[29] Khan U, May P, ÓNeill A, Coleman JN. Development of stiff, strong, yet tough composites by the addition of solvent exfoliated graphene to polyurethane. Carbon 2010;48:4035–41. http://dx.doi.org/10.1016/j.carbon.2010.07.008.
[30] Gong L, Kinloch IA, Young RJ, Riaz I, Jalil R, Novoselov KS. Interfacial stress transfer in a graphene monolayer composite. Adv Mater 2010;22:2694–7. http://dx.doi.org/10.1002/adma.200904264.
[31] Wang X, Xing W, Zhang P, Song L, Yang H, Hu Y. Covalent functionalization of graphene with organosilane and its use as a reinforcement in epoxy composites. Compos Sci Technol 2012;72:737–43. http://dx.doi.org/10.1016/j.compscitech.2012.01.027.
[32] Kuila T, Bose S, Mishra AK, Khanra P, Kim NH, Lee JH. Effect of functionalized graphene on the physical properties of linear low density polyethylene nanocomposites. Polym Testing 2012;31:31–8. http://dx.doi.org/10.1016/j.polymertesting.2011.09.007.